A modeling approach for the purification of group III metals (Ga and In) by zone refining

K. Ghosh, V. N. Mani, and S. Dhar

Citation: Journal of Applied Physics **104**, 024904 (2008); doi: 10.1063/1.2959832
View online: http://dx.doi.org/10.1063/1.2959832
View Table of Contents: http://scitation.aip.org/content/aip/journal/jap/104/2?ver=pdfcov
Published by the AIP Publishing

A modeling approach for the purification of group III metals (Ga and In) by zone refining

K. Ghosh,[1,a)] V. N. Mani,[2] and S. Dhar[1]
[1]*Department of Electronic Science, University of Calcutta, 92 A. P. C. Road, Kolkata 700009, India*
[2]*Ultra-pure Materials Division, Centre for Materials for Electronics Technology (C-MET), IDA Phase-III, Cherlapally, HCL (Post), Hyderabad 500051, India*

(Received 14 January 2008; accepted 2 June 2008; published online 29 July 2008)

An "experimental friendly" model for zone refining process is proposed which predicts effective zone length in each refining passes that would lead to maximal solute removal, thereby leading to ultrapurification of the material for use in high-end electronic applications. The effectiveness of the model is experimentally tested and validated by purifying gallium from 4N (99.99%) to 6N5 (99.99995%) purity level at 30% yield and ~6 N at 70% yield with respect to targeted metallic impurities such as, Zn, Cu, Al, Ca, Bi, Si, Pb, Ni, Mn, and Fe, as analyzed by inductively coupled plasma optical emission spectrometry, graphite furnace atomic absorption spectrometry, and high resolution inductively coupled plasma mass spectrometry techniques. The distribution coefficient (k) of all the targeted impurities, detected in the purified gallium, was found to be less than 1. By comparing the experimentally obtained axial concentration profiles with the theoretical calculations, the k values of some detected impurities, such as Ca and Al, are determined to be ~0.8, Pb and Bi to be 0.7, Cu to be 0.65, and Fe to be 0.68, which prove the efficiency of the proposed model in reducing the concentration of these vulnerable impurities significantly. Following the model and as evidenced from the theoretical predictions, degradation of material purification containing a mixture of impurities having k less than as well as greater than 1 was elucidated experimentally by zone refining of 4N6 indium. Only a 40% yield of 5N6 indium was obtained, thereby highlighting the intricacies and problem areas in ultrapurification of these types of material. © *2008 American Institute of Physics*. [DOI: 10.1063/1.2959832]

I. INTRODUCTION

Production of III–V electronic materials require ultrahigh pure starting materials with purity exceeding 6N (99.9999%) levels, wherein the total concentration of impurities is less than 1 ppm. For example, ultrahigh pure gallium is used as the starting material for growing high quality GaAs single crystals, which have applications in electronic and optical devices, such as high speed integrated circuits (ICs), optoelectronic ICs, and efficient light detectors and emitters. Similarly, ultrahigh pure indium is also used to grow InP single crystals that are used as substrates for the fabrication of InP based photodiodes and lasers used in optical communications. Impurity density in these starting materials can be reduced to significantly low levels by establishing a molten zone in the material ingot, which is moved from one end to the other, one or more times at a controlled rate and temperature. This process is known as zone refining, which is extensively used for material purification, as described by Pfann.[1] In multipass zone refining, a series of closely spaced heaters forming a number of molten zones traverses the charge in a single operation. In this technique, time can be saved as succeeding crystallization begin before the completion of the first one. A number of research works were carried out based on ultrapurification of materials by zone refining.[2–9] Figure 1 shows the zone refining and normal freezing operation principles. Normal freezing is the elemental step in the method of purification by repeated fractional crystallization. In this process, the whole material ingot is first melted, which is then slowly frozen from one end.

Material purification by zone refining also depends on the type and concentration of the impurities that are present in the starting material. The efficiency of zone refining in segregating the impurities depend on the distribution coefficient k, which is defined as

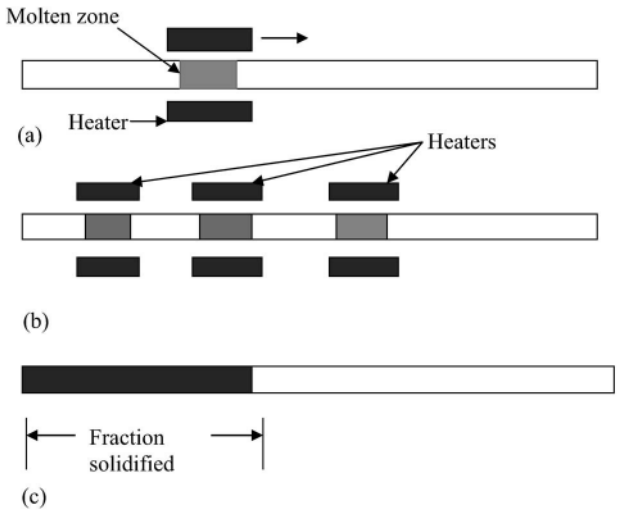

FIG. 1. Schematic sketch of zone melting operation for (a) single pass zone refining, (b) multipass zone refining, and (c) normal freezing.

a)Electronic mail: kaustab_ghosh2002@yahoo.co.in.

$$k = C/C_L, \tag{1}$$

where C is the solute concentration in the freezing solid at solid-liquid interface and C_L is the solute concentration in the main body of the liquid zone. For $k<1$, the solute or the impurity is rejected by the solidifying interface into the molten zone, whose concentration is thus reduced at the head end and an enriched layer builds up ahead of the interface at the tail end. A similar argument applies for $k>1$ except that a depleted rather than an enriched layer builds up. Impurities having k values close to 1 are difficult to segregate.

Another important parameter contributing to the efficiency of purification is zone length, which has been studied in detail by many researchers.[10–17] Davies *et al.*[10] found in their studies that the ratios of optimum zone length to ingot length for the first and second passes are 1 and 0.3, respectively. Ho *et al.*[11,12] found out optimal zone lengths for maximum separation up to ten passes and optimal variation of zone lengths in multipass zone refining processes. Spim *et al.*[13] developed a numerical model that is capable of predicting solute redistribution at any stage of a multipass zone refining process and also suggested that effective refining operation is possible by restricting the molten zone length to $0.2L$ for initial three zone passes, followed by $0.1L$ up to six passes and $0.05L$ for passes greater than six, where L is the length of the ingot.

Experimental process modeling provides valuable information and insights into the control and optimization of the parameters. The feedback and the results obtained from the study help in affecting necessary and required modifications. In zone refining, the results of the study enable one to select optimal number of passes, zone length, temperature gradient, sample, and crucible dimensions so as to improve the purification efficiency and to increase the purity level. However, in spite of extensive theoretical and experimental research activities, such a detailed modeling treatment specifically suited to the purification system and experimental refining conditions meant for ultrapurifying the group III metals is seldom available in literature. In the light of the above situation, a process modeling approach for zone refining of group III metals has been proposed. The model is based on the effective zone length that maximally reduces the impurity concentration at each refining pass. A numerical model has been used to map the impurity distribution along the refined ingot and to elucidate their segregation behavior based on their distribution coefficient. To investigate the efficiency of the proposed model, experimental purification work was carried out using 4N pure gallium and 4N6 pure indium as the starting material, following and maintaining the effective zone length for each pass, as described by the model. After 50 refining cycles, axial impurity profiles were analyzed and compared with the theoretical results to validate the predictions and to elucidate the impurity distribution characteristics and purity level of the refined materials.

A. Numerical and process modeling of zone refining operation

The following assumptions were made in deriving the equations of solute (impurity) distribution for single and repeated unidirectional zone passes.

(1) The distribution coefficient k is constant throughout.
(2) Zone length and travel rate are constant in each pass.
(3) Uniform composition in the liquid.
(4) Negligible solid-liquid density differences.
(5) Negligible diffusion in the solid.

In the model, the material ingot is divided into 100 equally spaced segments of width dx and we assumed a uniform initial solute concentration C_0 for all segments. The equation for the solute distribution along the ingot after a single refining pass, as proposed by Pfann,[1] is given by

$$C(1,X)/C_0 = 1 - (1-k)\exp(-kX/Z), \tag{2}$$

where $X=x/L$ is the normalized distance from the starting end of the ingot, x is the distance from starting end of the ingot, $Z=l/L$ is the normalized molten zone length, and l is the length of the molten zone.

Equation (2) is valid for all parts of the ingot except for the last zone, i.e, at $x=L-l$, where normal freezing occurs. The solute distribution in this last portion of the sample is given by Scheil,[18]

$$C(1,X)/C_0 = \{1-(1-k)\exp[-k(1-Z)/Z]\} \times \{1-[X-(1-Z)]/Z\}^{k-1}. \tag{3}$$

However, according to Ho *et al.*,[11] maximum solute removal for the first pass is achieved when the zone length is equal to the ingot length, i.e, normal freezing, which is the same as the result obtained by Davies,[10] and the concentration distribution is given by

$$C(1,X)/\mathrm{Co} = k(1-X)^{k-1}. \tag{4}$$

However, single pass operation is not sufficient to obtain higher ultrapurification of material. In order to obtain the material in its ultrahigh pure form, the material ingot should be subjected to repeated and optimal number of unidirectional passes depending on the type, nature of targeted impurities, and other experimental conditions. The model of Spim *et al.*[13] was used to encompass the impurity distribution for repeated number of passes along three different regions of the ingot.

(i) At

$$X = 0, \quad C(n,0) = k(dx/Z)\left[\sum_{i=0}^{M-1} C(n-1,idx)\right], \tag{5}$$

where M is the number of individual elements of length dx inside the volume of the normalized molten zone length Z and n is the number of zone passes.

(ii) At

$$0 < X \le 1-Z, \quad C(n,X) = C(n,X-dx) + (kdx/Z) \times [C(n-1,X+Z-dx) - C(n,X-dx).] \tag{6}$$

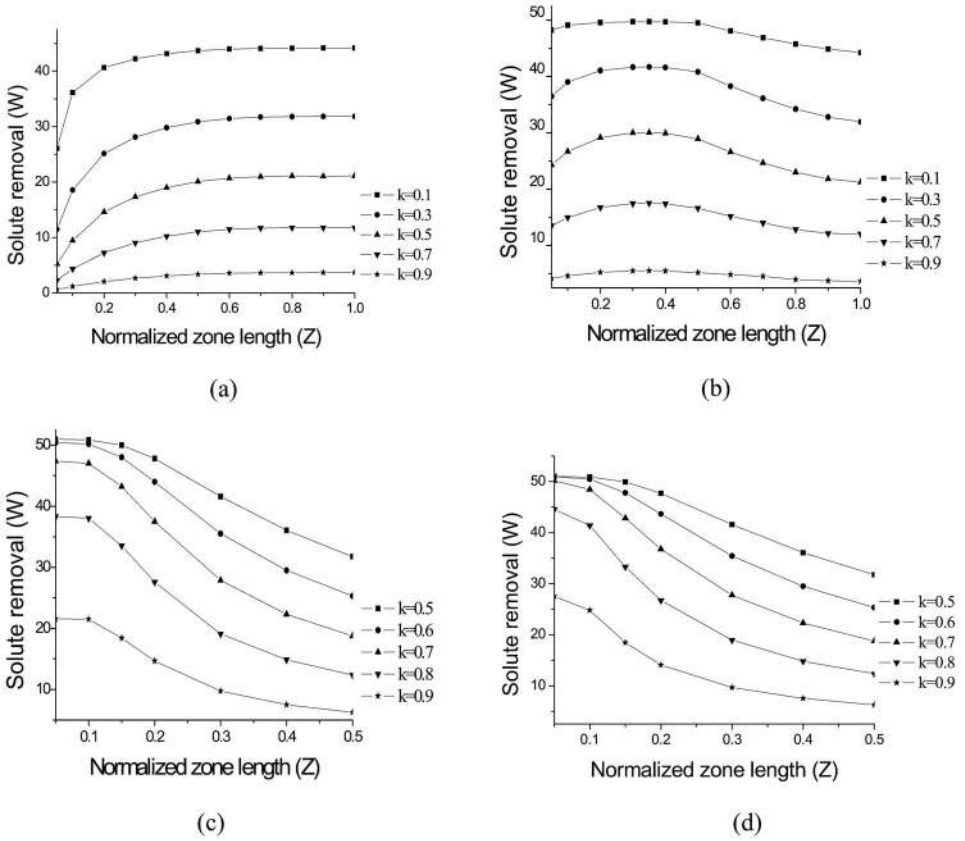

FIG. 2. Effect of the zone length on solute removal after (a) single refining pass, (b) second pass, (c) 30 passes, and (d) 50 passes, with the previous passes operated by effective the zone length that led to maximum solute removal.

(iii) At

$$1 - Z < X < 1, \quad C(n,X) = k(1-X)^{k-1}(Z^{-k})\left[1 - dx\sum_{X=0}^{1-Z} C(n,X)\right]. \tag{7}$$

In this region, the zone length is no longer constant and the impurity is not taken in.

The solute or impurity removal W_n for each refining pass is given by

$$W_n = \sum_{X=0}^{0.5} [1 - C(n\,.\,X)] \quad \text{for} \quad k < 1, \tag{8}$$

$$W_n = \sum_{X=0}^{0.5} [C(n,X) - 1] \quad \text{for} \quad k > 1. \tag{9}$$

The higher the value of the solute removal in a particular refining pass, the higher the purification efficiency of the material subjected to the refining process. The reported k values of most of the impurities in group II and III metals are less than1 and very few of them have $k>1$.[19] Hence, the zone refining process model describing suitable zone length for each refining pass for maximum solute removal and yield was based on the consideration that all the impurities in the material have $k<1$ up to 0.9. After selecting the suitable and effective zone length for each pass that leads to maximum solute removal, the numerical model was used to consider the effect of the impurities having $k>1$ on the purification efficiency, which is discussed elsewhere in this paper.

The numerical results explaining the effect of normalized zone length (Z) on solute removal (W_n) having different solute distribution coefficients from 0.1 to 0.9 for different passes is shown in Fig. 2. Figure 2(a) shows the same after single pass of the molten zone. It is seen that the solute removal increases with an increase in the length of the molten zone. Maximum solute removal can be obtained under normal freezing operation, i.e., when, $Z=1$, which is in agreement with the findings of Davies.[10] For the second pass, maximum solute removal can be obtained by reducing Z to 0.35 with the first pass operated under normal freezing conditions, as shown in Fig. 2(b). In this manner, the effective values of Z for each pass and up to 20 passes were computed and tabulated in Table I, where the previous passes were operated under the effective value of Z that led to maximum removal of the impurities (solutes). To clearly distinguish the effect of normalized molten zone length on solute removal, the enlarged portions of Figs. 2(a) and 2(b) for $k=0.5$, 0.1, and 0.9 are shown in Fig. 3.

It is observed from Table I that a decrease in molten zone length with an increase in the number of zone passes

TABLE I. Effective zone length for each pass for maximum solute removal-proposed zone refining process model.

No. of Passes	1	2	3	4	5–8	9–19	20 and greater passes
Normalized Molten zone Length	1	0.35	0.25	0.2	0.15	0.1	0.05

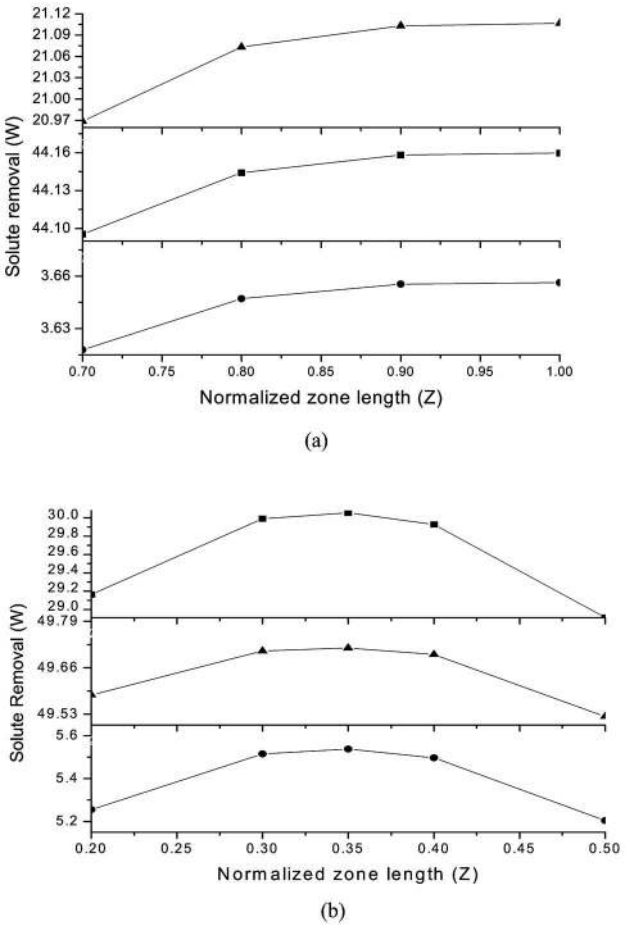

FIG. 3. Enlarged portion for $k=0.5$, 0.1, and 0.9 (respectively from top to bottom) of Figs. 2(a) and 2(b) to clearly distinguish the effect of normalized molten zone length upon solute removal.

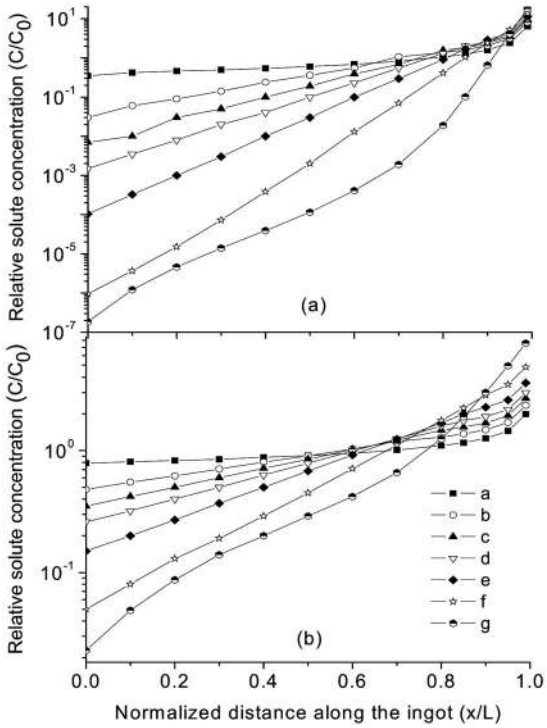

FIG. 4. Concentration profile of impurity having (a) $k=0.4$ after 30 passes, (b) $k=0.8$ after 50 passes with different refining approaches. Symbols used: a, continuous normal freezing for all passes; b, 1st pass-normal freezing, $Z=0.35$ for 2nd pass and maintained for $n>2$; c, same as b up to 2nd pass and then $Z=0.25$ for 3rd pass and maintained for $n>3$; d, same as c up to 3rd pass and then $Z=0.20$ for 4th pass and maintained for $n>4$; e, same as d up to 4th pass and then $Z=0.15$ for 5th pass and maintained for $n>5$; f, same as e up to 8th pass and then $Z=0.10$ for 9th pass and maintained for $n>9$; g, same as f up to 19th pass and then $Z=0.05$ for the 20th pass and maintained for $n>20$; and (-) proposed zone refining process model.

favors maximal reduction in the solute concentration. In the 20th pass, Z reduced to 0.05. The model has been developed in order to suit the available system and the experimental refining conditions; further reduction in Z was not done since it becomes difficult to maintain narrow zone length experimentally in view of instrumentation complexities. Hence, for higher number of passes ≥ 20, Z is to be maintained at 0.05. Figures 2(c) and 2(d) show the effects of different normalized zone lengths (Z) on the solute removal (W_n) after 30 and 50 passes. From Fig. 2(c), it is seen that W_n increases with a decrease in the value of Z up to 0.1, after which there is a slight increase in W_n at 0.05. Similar trend is exhibited in Fig. 2(d) except that there is significant increase in W_n at $Z=0.05$ as compared to that at 0.1. This theoretical observation also suggests that with the increase in the number of passes, shorter zone length enhances impurity solute removal and thus aids in improving the purity of the material.

The zone refining process model, as presented in Table I, describes an effective material purification approach by decreasing the zone length with an increase in the number of passes. For the first pass, maximum solute removal is affected with $Z=1$ or normal freezing operation. Similarly, W_n becomes maximum at $Z=0.35$ in the second pass and likewise the value of Z decreases for higher number of passes. However, it is important to compare the effects of the distribution of impurities along the ingot if the zone length is not decreased, as shown in Table I; i.e., if $Z=1$ or normal freezing operation is maintained for all 50 passes or if $Z=1$ for the first pass and $Z=0.35$ for the 2nd pass and maintained for $n>2$ up to 50 passes and likewise continuing in this manner until the proposed process model is approached. Figure 4 shows the comparison of all these approaches and it is seen that best possible reduction in the impurity concentration can be obtained by the method as regulated by the proposed model. The predicted solute concentration profile along the ingot following this model is compared with the technique of Spim *et al.*[13] in Figs. 5(a) and 5(b), where the proposed model indicates a slight improvement in reducing the solute concentration in the purest region of the ingot.

Ho *et al.*[11] presented an the approach to evaluate the optimal zone length for maximum solute removal W_n for each subsequent refining passes. However, their approach is purely based on theoretical predictions and the optimal zone length for each pass varies with the values of the distribution coefficient k. The materials to be purified by zone refining contain of a variety of impurities having different k values. The optimal zone length for maximum reduction in the concentration of all these impurities, calculated using the method of Ho *et al.*,[11] cannot be applicable and used for this purpose since it varies with the value of k. The modeling approach proposed in this paper was developed for experi-

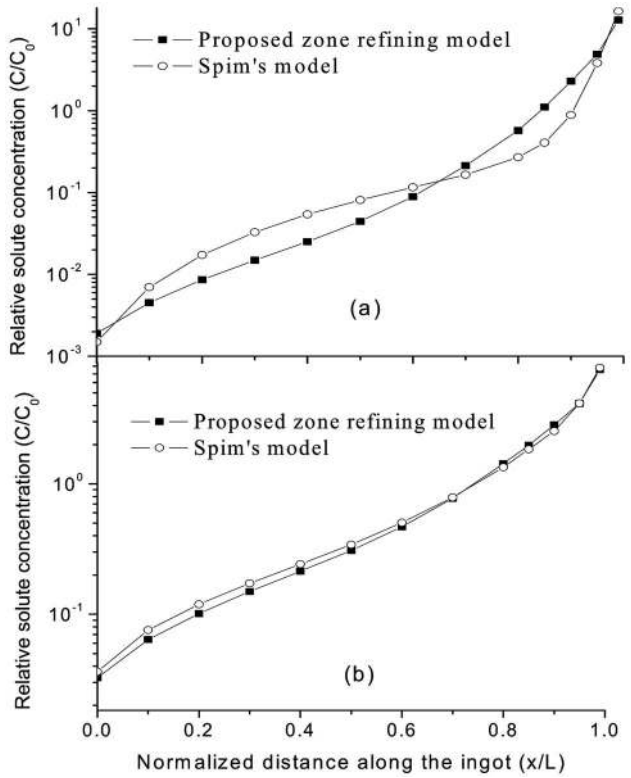

FIG. 5. Comparison of the proposed model with the model of Spim *et al.* (Ref. 13) for (a) $k=0.4$ after 10 passes (b) $k=0.8$ after 20 passes.

mental validation and application and can be used for maximally reducing the concentration of all the impurities having $k \leq 0.9$.

II. EXPERIMENTAL PROCEDURE

Gallium of 4N and indium of 4N6 purity were purified using a laboratory scale vertical zone refiner (Instrolec 200),[6] which is specifically suitable for refining low melting point materials. The system consists of nine separate heaters and eight coolers along the length to produce nine narrow molten zones in the material to be refined. The coolers serve to confine the molten zones produced by the heaters and also help to obtain rapid and good crystallization from the melt. The material was loaded in a polymeric glass composite based tube of 14 mm diameter and 650 mm length and also sealed at both ends with air-tight corks under class 100 clean room environment. This sample tube was moved vertically upward passing through the heater/cooler assembly at a fixed rate of 5 mm/h. Thus, the sample was processed more quickly than moving it through a single heater down the entire length, although final refining effects the remaining same. As the molten zone traversed the entire length of the tube, a cam-wheel setup automatically moved back the tube to the initial position to start the next refining cycle.

To start the first pass by normal freezing operation, the material (gallium or indium) in the sample tube was entirely melted and placed in the refining system. All heaters were switched off and the coolers were switched on, and the coolant flow was regulated to freeze the molten material at the controlled rate. The optimized zone length for higher number of zone passes was maintained and monitored by adjusting the temperature of the heaters controlled by a control switch having an accuracy of ± 1 °C. After completing 50 refining cycles, 5 g samples taken from the original starting raw material and the refined portions of the ingot were placed in a polypropylene vial. These were dissolved in 10 ml of 69% HNO_3 and were transferred to a volumetric flask to be diluted with 100 ml of high purity water. This solution was used for the subsequent inductively coupled plasma optical emission spectrometry (ICP-OES), graphite furnace atomic absorption spectrometry (GFAAS), and high resolution inductively coupled plasma mass spectrometry (HR-ICPMS) analyses.

III. RESULTS AND DISCUSSIONS

A. Theoretical prediction of total impurity concentration distribution

During purity evaluation of materials for use in electronic applications, the total concentration of impurities needs to be considered below the desired benchmark level. In zone-refined materials, the total concentration of impurities in the purified portion of the ingot should be below 1 ppm in order to be claimed as 6N pure. In the base matrix of the material, a variety of impurities are homogenously mixed having different k values. Higher purification efficiency can be achievable for materials containing impurities having k values either less than or greater than 1 since it can easily be purified due to reduction in the impurity concentration at one end with gradual accumulation at the other. For materials containing both types of impurities, i.e., some have $k<1$ and the rest have $k>1$, the total concentration reduction in the impurities having $k<1$ at one end of the ingot is hampered by the accumulation of the impurities at the same end having $k>1$. Thus, these types of materials are difficult to purify. Hence, for the following two types of materials, computations were carried out for theoretical understanding and predicting the impurity concentration distribution after 50 passes:

(1) materials containing all impurities having $k<1$ and
(2) materials containing some impurities having $k<1$ and the rest having $k>1$.

For the material of the first type, the computed concentration profiles of different impurities having $k<1$ mixed with $k=0.5$ and $k=0.7$ impurity along the refined material ingot is depicted in Figs. 6(a) and 6(b), respectively. Here, just as described, higher purification efficiency of the material is exhibited with reduced total impurity concentration at one end and accumulated concentration at the other. From Fig. 6(a), it is also seen that lower the value of k less than unity, the more is the impurity concentration reduction at the purest end except that the same reduction trend is observed for $k=0.5$ mixed with $k=0.1$ and with $k=0.3$ impurity at this end. Figure 6(b) shows similar kind of observation with the same impurity concentration reduction trend for $k=0.7$ mixed with $k=0.1$, 0.3 and 0.5 impurities. This shows that, after 50 passes, the impurities having lower distribution coefficients, i.e, $k=0.1$, 0.3, and 0.5, reach a steady state or

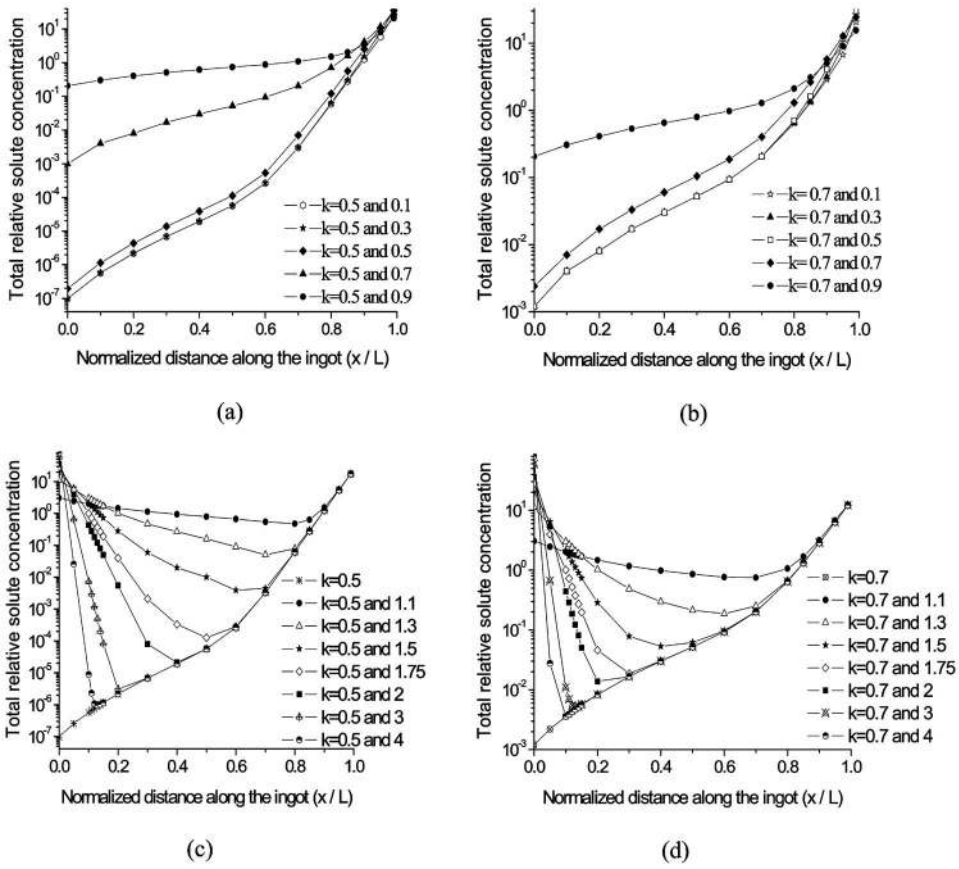

FIG. 6. Effect on impurity concentration profiles having $k<1$ along the ingot after 50 passes (a) on the impurity having $k=0.5$, (b) on the impurity having $k=0.7$, and the same for $k>1$, (c) on the impurity having $k=0.5$, and (d) on the impurity having $k=0.7$.

ultimate distribution representing maximum attainable separation, where the forward convective flux of the impurity due to freezing interface at all points in the ingot is opposed by an equal backward flux due to the molten interface.

For the second type of material, Figs. 6(c) and 6(d) depict the concentration profile of impurities having $k>1$ mixed with impurity having $k=0.5$ and $k=0.7$, respectively. Contrary to the observations in Figs. 6(a) and 6(b), it is seen that for these materials, the purification efficiency and yield are lowered due to the accumulation of impurities at either ends of the ingot, making the total impurity concentration unaffected and a major reduction in the total concentration occurs at the intermediate region. It is also seen that higher the value of k above unity, the more is the reduction in total impurity concentration in the purest region. Figures 6(a)–6(d) also illustrate that impurities having distribution coefficients much greater or less than unity easily gets segregated and reduced in concentration in the purest portion compared to the segregation behavior of impurities having distribution coefficient close to unity. Thus, this reinforces the statement that vulnerable impurities are those having $k \sim 1$ and cannot be segregated easily.

B. Comparison and correlation: Theory with experimental analysis results

It was found from our earlier experiments[5–7] and also from published reports[2,19] that the impurities in gallium have $k<1$ and indium consist of impurities having $k<1$ as well as $k>1$. Hence, to validate the theoretical findings and to test the efficiency of the proposed refining model, 4N pure gallium and 4N6 pure indium were zone refined for the same number of passes. Higher number of passes was carried out to ensure that the impurities having $k \sim 1$ ($k=0.8$, 0.9 or 1.1, 1.2, etc.) are also significantly reduced in concentration for ultrapurification of the material.

Table II shows the impurity analysis by ICP-OES, GFAAS, and HR-ICPMS of refined gallium samples, where sample 1 (at $X=0.1$) was taken from the starting end of the ingot and sample 5 (at $X=0.9$) was taken from the other end. Different analysis techniques (ICP-OES, GFAAS, and HR-

TABLE II. Concentration of impurities in raw and refined gallium samples analyzed by ICP-OES, GFAAS, and HR-ICPMS after 50 refining passes in ppm. ND-not detected. N.B.: limit of detection for Zn and Si by HR-ICPMS=0.008 ppm; limit of detection of Mn by HR-ICPMS =0.005 ppm; and limit of detection for Ni by HR-ICPMS=0.002 ppm.

Elements	Raw gallium	Sample 1	Sample 2	Sample 3	Sample 4	Sample 5
Zn	57.0	ND	ND	ND	ND	145.7
Cu	12.0	0.05	0.13	0.18	0.28	56.7
Pb	21.0	0.24	0.32	0.72	0.98	33.5
Bi	1.65	0.031	0.045	0.1	0.5	2.62
Fe	2.1	0.03	0.045	0.06	0.1	7.58
Ni	0.1	ND	ND	ND	0.05	0.34
Ca	0.5	0.02	0.1	0.2	0.41	1.76
Al	0.5	0.03	0.05	0.12	0.38	1.78
Mn	0.5	ND	ND	ND	0.2	2.0
Si	5.0	ND	ND	ND	ND	24.8
Total Conc.	100.35	0.401	0.69	1.38	2.9	276.78

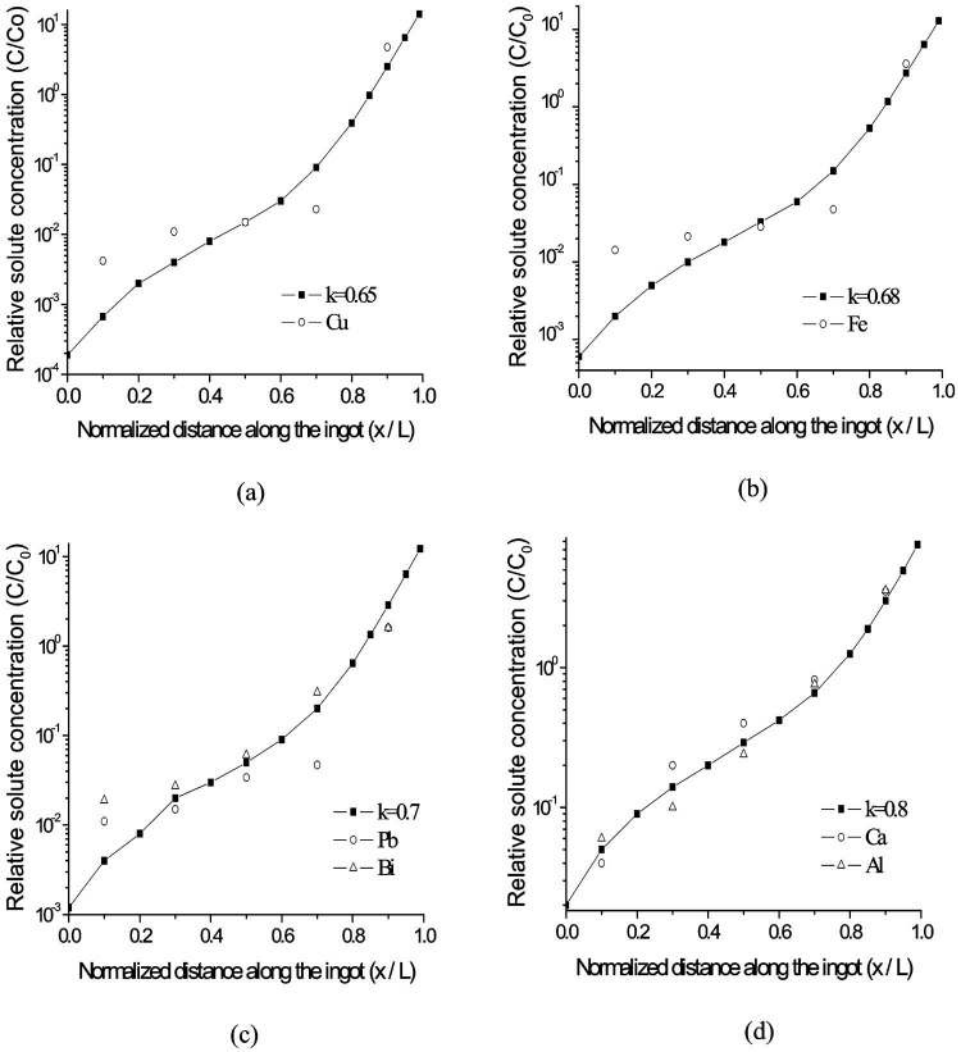

FIG. 7. Comparison of concentration distribution of (a) copper (b) iron (c) lead and bismuth, and (e) aluminum and calcium with the theoretical distribution after 50 passes.

ICPMS) were used to detect lower impurity concentration in which HR-ICPMS can detect to a minimum of 0.001 ppm. From Table II, it is seen that the major impurities in 4N pure starting raw gallium metal were Zn, Cu, Pb, Bi, Fe, Ni, Ca, Al, Mn, and Si, and the total concentration of these impurities maximally reduced in sample 1 and accumulated in sample 5 indicates that for all these impurities, $k<1$. The concentration of Zn and Si is significantly reduced below the detection limit (0.008 ppm) in samples 1–4 from initial concentrations of 57 and 5 ppm, respectively, indicating that their distribution coefficient in Ga is much below unity. The initial concentration of Ni and Mn in 4N pure starting raw gallium was in traces, i.e., 0.1 and 0.5 ppm, which was reduced below the detection limit (0.005 ppm for Mn and 0.002 ppm for Ni) in samples 1–3. However, 0.05 ppm of Ni and 0.2 ppm of Mn were detected in sample 4. This suggests that the distribution coefficient of these impurities though less than unity has higher value than that of Zn and Si. Higher initial concentration of these impurities may have detrimental effect on material purification. The experimental segregation behavior of the rest of the detected impurities, such as Cu, Pb, Bi, Fe, Al and Ca, was compared with the calculated concentration profiles, as shown in Fig. 7. From the figure, it is seen that the concentration profile of Cu and Fe is in close agreement with the computed segregation trend exhibited by impurity having k values of 0.65 and 0.68, respectively, Pb and Bi both follows the trend exhibited by $k=0.7$, and Al and Ca both follows the trend of $k=0.8$. Thus, the comparison shows that most of the detected impurities in gallium have high k values, i.e., $0.65 \leq k \leq 0.8$. However, still with this effective refining technique, the total concentration of impurities is reduced from 100.35 ppm to 0.401 ppm in sample 1 and 0.69 ppm in sample 2. The total concentration in samples 3 and 4 also reduced to 1.38 and 2.9 ppm. Also, 30% of the purest portion of the ingot (mean total concentration of samples 1 and 2) was purified up to 0.55 ppm, i.e., (~6*N*5 or 99.999 95% pure) and 70% of the ingot (mean total concentration of samples 1, 2, 3, and 4) was purified up to 1.3 ppm, which is almost 6N pure. Thus, this high material purification and yield prove the efficiency of the refining model.

Table III shows the impurity analysis of refined indium samples by ICP-OES. Samples 1 and 3 are mean analysis results of a number of samples taken from 30% of the ingot at opposite ends, whereas sample 2 is the mean result taken from middle 40% of the ingot. From the table, it can be seen that most of the impurities, such as Zn, Cu, Ag, Sn, Fe, and Ge were accumulated in sample 3 and reduced in concentra-

TABLE III. ICP-OES analysis of indium samples after 50 refining passes in ppm. N.B.: limit of detection of ICP-OES is 0.1 ppm.

Elements	Raw indium	Sample 1	Sample 2	Sample 3
Zn	6.4	0.79	1.61	18.85
Pb	1.0	1.6	ND	ND
Te	2.6	6.14	ND	ND
Fe	5.6	ND	0.7	7.15
Sn	9.58	ND	ND	15
Cu	6.5	ND	0.2	10.5
Mg	5.8	12.66	1.83	0.98
Ag	1.0	ND	ND	1.5
Ge	1.5	ND	ND	3.7
Total	39.98	21.19	4.34	57.68

tion in sample 1, indicating that the distribution coefficient of these impurities is less than unity. The opposite effect was observed for Pb, Te, and Mg which suggests that they have $k>1$ in indium. As predicted from Figs. 6(c) and 6(d), the impurities accumulated at both ends of the ingot and greater purification of the material was obtained in the middle region in sample 2, thus validating the theoretical representation. Since concentration reduction in one type of impurity ($k<1$) is hampered by the accumulated concentration of the other type ($k>1$), higher resolution analysis techniques such as HR-ICPMS was not used to detect lower impurity concentration. Hence, based on the detection limit of ICP-OES of 0.1 ppm, the total concentration of impurities is reduced from 39.98 ppm (4N6) to 4.34 ppm (5N6) in the purest portion of the ingot (sample 2) at a yield of 40%.

IV. CONCLUSION

A zone refining process modeling has been described which is based on the zone length optimization for maximum solute removal in each pass. The utility and effectiveness of the proposed model were interpreted and correlated with reference to existing modeling approaches. A study was also made on the segregation characteristic of selected impurities that are homogeneously mixed and coexisting in the base matrix of the material subjected to the refining process. To validate our results and findings, experiments were conducted on 4N pure gallium, which was purified to 6N5 level at 30% yield and near to 6N at 70% yield, containing some impurities having distribution coefficient in the range of $0.65 \leq k \leq 0.8$. However, even with this technique, ultrapurification of materials containing mixture of impurities having k less than as well as greater than 1 is difficult, which is justified by purifying indium from 4N6 to 5N6 level with a yield of 40% with similar process concepts applied for purifying gallium. The experimental results were interpreted and correlated with the theoretical predictions.

ACKNOWLEDGMENTS

The authors would like to acknowledge the financial support provided by DRDO in sponsoring a major project and also wish to thank Dr. M. A. Reddy and Dr. K. Chandrasekaran of CCCM for chemical analysis of gallium samples and Dr. G. Anil, Scientist, C-MET, for chemical analysis of some samples of gallium and indium. The authors would also like to thank Dr. R. Muralidharan, Scientist G and Dr. A.K. Garg, Scientist-F, SSPL for their useful suggestions and discussions.

[1]W. G. Pfann, *Zone Melting*, 2nd ed. (Wiley, New York, 1964).
[2]A. B. I. Bollong, R. P. Bult, and G. T. Proux, U.S. Patent No. 4,888,051 (1989).
[3]G. B. Feldewerth, A. B. I. Bollong, and D. C. Bunnell, U.S. Patent No. 5,513,834 (1996).
[4]R. P. Bult, A. B. I. Bollong, and R. F. Redden, U.S. Patent No. 4,690,725 (1987).
[5]V. N. Mani and K. Balaraju, Met., Mater. Processes **18**, 107 (2006).
[6]V. N. Mani and K. Balaraju, Proceedings of the International Workshop on Preparation and Characterization of Technologically Important Single Crystals, India, 2001 (unpublished), p. 177.
[7]K. Ghosh, S. T. Ali, and V. N. Mani, *Advances in Technologically Important Crystals* (Macmillan, India, 2006), p. 569.
[8]S. T. Ali, R. C. Reddy, N. R. Munirathnam, C. Sudheer, G. Anil, and T. L. Prakash, Sep. Purif. Methods **52**, 288 (2006).
[9]G. Anil, M. R. P. Reddy, D. S. Prasad, S. T. Ali, N. R. Munirathnam, and T. L. Prakash, Mater. Charact. **58**, 92 (2007).
[10]L. W. Davies, Trans. AIME **215**, 672 (1959).
[11]C. D. Ho, H. M. Yeh, and T. L. Yeh, Sea Technol. **6**, 227 (1996).
[12]C. D. Ho, H. M. Yeh, and T. L. Yeh, Sep. Purif. Technol. **15**, 69 (1999).
[13]J. A. Spim, M. J. S. Bernadou, and A. Garcia, J. Alloys Compd. **298**, 299 (2000).
[14]K. A. Jackson and W. G. Pfann, J. Appl. Phys. **36**, 320 (1965).
[15]G. H. Rodway and J. D. Hunt, J. Cryst. Growth **97**, 680 (1989).
[16]H. M. Yeh and W. H. Yeh, Sep. Sci. Technol. **14**, 795 (1979).
[17]C. D. Ho, H. M. Yeh, and T. L. Yeh, J. Chin. Inst. Chem. Eng. **27**, 395 (1996).
[18]E. Scheil, Z. Metallkd. **34**, 70 (1942).
[19]J. Drapala, L. Kuchar, and G. S. Burkhanov, Inorg. Mater. **34**, 165 (1998).